ELECTRON BACKSCATTER DIFFRACTION ANALYSIS OF THE EARLIEST-FORMED SOLIDS IN THE SOLAR SYSTEM P. Mane[1], S. Wallace[2], P. Wallace[1], K. Domanik[1], and T. J. Zega[1,3], [1] Lunar and Planetary Laboratory, University of Arizona, Tucson, AZ, 85721 (email: pmane@lpl.arizona.edu), [2]EDAX, Ametek, Materials Analysis Division, Mahwah, NJ, 07430. [3]Dept. of Materials Science and Engineering, University of Arizona, Tucson, AZ 85721.

Introduction: Calcium-Aluminum-rich Inclusions (CAIs) are some of the earliest-formed solids in the Solar System [1,2]. Their fabric and microtextures contain information on the earliest chemical and physical events that occurred in our Solar System. Electron Backscatter Diffraction (EBSD) is a fast and most reliable way to acquire data for crystalline structure and orientation in a solid crystalline phase and analyze such fabric and microtextures [3]. Unlike optical techniques, it is possible to acquire data for phases of all symmetries (including isotropic phases) and for opaque phases.

EBSD data give true 3-dimensional orientations for individual crystals, which is superior to optical pole figures which give 2-dimensional orientations. The spatial resolution can be sub-microns, which is superior to resolution attainable using selected-area electron-diffraction techniques. EBSD data acquired using either a scanned electron beam, or an automated stage and a stationary electron beam can include analyses of thousands of individual grains within minutes to hours, and acquisition of data for millions of individual spots in a single one-day run is routine. By applying this powerful technique to CAIs to determine their fabric and textures, our goal is to gain information about various early solar system processes experienced by CAIs such as condensation, melting, shock and parent body metamorphism.

Here we present EBSD data to determine the crystallographic orientation of melilite and spinel in the CAI and it's Wark-Lovering (WL) rim sequence.

Samples and Analytical Methods: We analyzed a type-A CAI (named as 'Hedgehog') from NWA 5028 (CR2 carbonaceous chondrite). Hedgehog contains melilite, spinel, perovskite as major mineral phases and also hosts opaque mineral assemblages. Hedgehog is surrounded by a Wark-Lovering (WL) rim sequence [4] containing an innermost hibonite + perovskite + spinel layer, followed by an intermediate melilite layer and the outermost pyroxene layer. The ^{26}Al-^{26}Mg relative age dating of the CAI and the WL rim suggests that the rim layer containing hibonite formed within ~640,000 years after the CAI formation [5].

The chemical and mineralogical characteristics of the CAI were studied using the Cameca SX100 electron microprobe at the Lunar and Planetary Laboratory. The X-ray maps were acquired at 1 μm/pixel resolution. Wavelength-dispersive-spectrometry was used to determine chemical composition of each mineral phase.

We used the FEI Helios NanoLAB 660 focused ion beam scanning electron microscope (FIB-SEM), at the Lunar and Planetary Laboratory, equipped with EDAX EDS (energy-dispersive spectroscopy) and EBSD detectors, to map areas of the CAI and the WL rim sequence for composition and grain orientation/structure. The section was mapped with a spatial resolution of 0.2 μm/pixel, to ensure that each (sub) grain was sufficiently sampled. The EBSD pattern from each point was indexed using the TEAM™ Analysis Software and OIM Analysis 8™ enabling the construction of pattern quality (IQ) maps, orientation maps, phase maps, and inverse pole figure plots of crystallographic orientation. The orientation data and pole figure plots were derived from selected areas of the CAI and its WL rims, each typically comprising several hundred thousand data points.

Results: Hedgehog has an elongated morphology (~2.9 mm × ~1.6 mm). The interior melilite occurs as blocky subhedral to euhedral crystals. The Åkermanite content on melilite varies, from Åk7 to Åk38. Individual melilite grains do not show compositional zoning, however Åk content decreases from the core towards the WL rim. Most melilite grains poikiolitically enclose spinel, perovskite, and metal grains.

Spinel grains are small, ranging in size from 10 to 60 μm, and have subhedral to euhedral morphologies. Some spinel grains form clusters that are concentrated in the center of the CAI and they are sparse or absent in the outer region of the inclusion; others are arranged in a shell-like structure, similar to those described as spinel palisade bodies [6]. Compositionally, spinels are unzoned and near-end member $MgAl_2O_4$. They contain minor TiO_2 (0.3 – 0.5 wt %) and Cr_2O_3 (0.1-0.4 wt %).

The EBSD data shows that almost all melilite grains in the interior of Hedgehog are severely deformed as seen in the color variation in the inverse pole figure (IPF) maps (Figure 1). The misorientation in the interior melilite grains are up to 30^0. In comparison, the rim melilite and spinel grains are much less deformed, as the fraction of melilite grains showing deformation is limited and the misorientations are $<10^0$. Spinel show much lower degree of heterogenous deformation. We used methods described in [7] to identify twins in spinels; both the interior and WL-rim contain minor twinned spinel grains.

Discussion: Shock experiments conducted on melilite at pressures ranging from 11 to 50 GPa report many

dislocations such as stacking faults, and amorphous lamellae with a width of the order of the unit cell dimensions [8]. All samples show presence of amorphous regions/diaplectic glass of melilitic composition, but no indication of morphological melting. They also exhibit many planar fractures [8]. In comparison, shock experiments on synthetic spinel conducted at 25.5 to 50 GPa reveal shock-induced dislocations with the Burger's vectors 1/2 <100> and abundant twin lamellae of the twin law {111}[9].

Deformation in CAI materials has been observed using transmission electron microscopy (TEM) previously [10-12]. Melilite grains from several type-A and type-B CAIs show high dislocation densities, deformation lamellae, and low-angle grain boundaries suggesting that these melilite grains are considerably strained. Baerber et al argued that high dislocation densities combined with absence of glass and fractures in melilite indicate mild shocks when the CAI was still hot [11]. Further, in many of these CAIs, spinel grains show dislocations with the Burger's vectors 1/2 <100>. No twin lamellae were observed in these spinels also suggesting that these minerals were already at high temperature when they were shocked (~1000c) [10].

In comparison, our data show that the material within rims and the inclusion both experienced shock processing, however, the interior melilite and spinel are severly deformed, whereas the rim melilite show only minor strain (Figure 1). Our EBSD data suggest that the mechanism that caused deformation in melilite was repetitive, and was specifically active before WL rim formation (<640,000 years), as the interior melilite seems to be much more deformed than the rim melilite.
Therefore, the melilites in the CAI deformed at in nebular settings. Shock processes in the early solar nebula similar those responsible for chondrule formation, could have been responsible for deformation in this CAI. As CAIs are more refractory than chondrules, this CAI did not undergo melting, however it was deformed during these events.

References: [1] Amelin Y. et al., (2010) EPSL, 300, 343-350. [2] Connelly J. N. et al., (2012) Science, 338(6107), 651-655. [3] D. J. Prior et al., (1999) American Mineralogist 84, 1741-1759. [4] Wark D. A. and Lovering J. F. (1977) LPSC VII, 95-112. [5]] Mane P. et al. (2016) 79th Annual Meeting of the Meteoritical Society, Abstract #1921. [6] Simon S. B. et al., (1997) MAPS, 32, 61-70. [7] Wright S. and Larsen R. (2002) Journal of Microscopy, 205, 245-252. [8] Schäfer H. et al., (1984) Physics and Chemistry of Minerals 10, 121-124. [9] Schäfer H. et al., (1983) Physics and Chemistry of Minerals 9, 248-252. [10] Muller W. and Wlotzka F. (1982) LPSC XII, 558-559. [11] Barber D. et al., (1984) GCA, 48, 769-783. [12] Greshake A. et al., (1998) MAPS, 33, 75-87.

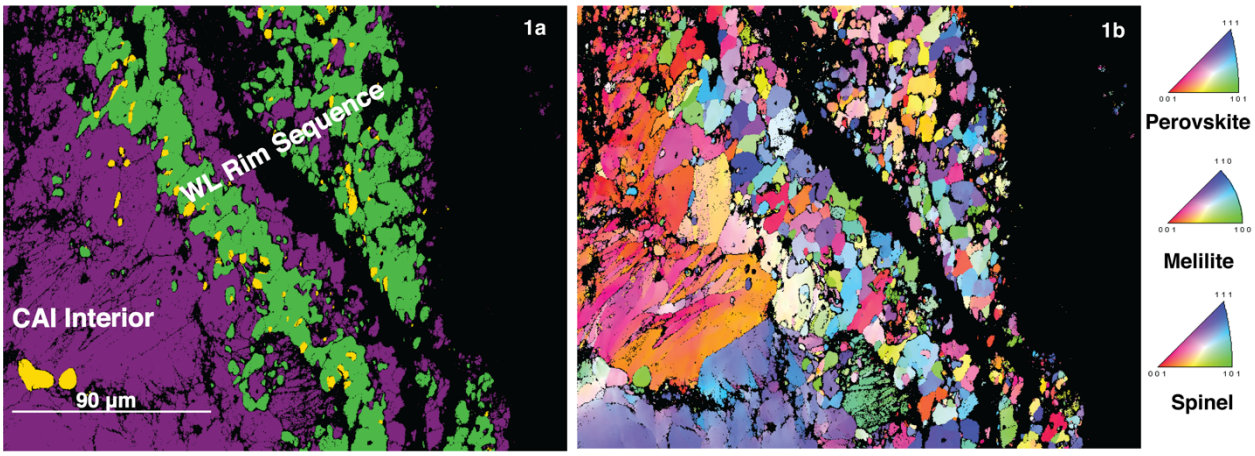

Figure 1. a. Phase map of a CAI and its WL rim showing melilite in purple; spinel in green and perovskite in yellow. b. Inverse pole figure maps of different mineral phases.